Surface-based Respiratory Motion Classification and Verification

Kerstin Müller[1], Christian Schaller[1], Jochen Penne[1], Joachim Hornegger[1]

[1]Chair of Pattern Recognition, Department of Computer Science, Friedrich-Alexander University Erlangen-Nuremberg, Martensstr. 3, 91058 Erlangen, Germany
christian.schaller@informatik.uni-erlangen.de

Abstract. To ensure precise tumor irradiation in radiotherapy a stable breathing pattern is mandatory as tumors are moving due to respiratory motion. Consequentially, irregularities of respiratory patterns have to be detected immediately. The causal motion of tissue also differs due to different physiological types of respiration, e.g., chest- or abdominal breathing. Currently used devices to measure respiratory motion do not incorporate complete surface deformations. Instead only small regions of interest are considered. Thereby, valuable information to detect different breathing patterns and types are lost. In this paper we present a system that uses a novel camera sensor called Time-of-Flight (ToF) for automatic classification and verification of breathing patterns. The proposed algorithm calculates multiple volume signals of different anatomical regions of the upper part of the patient's body. Therefore disjoint regions of interest are defined for both, the patient's abdomen and thorax. Using the calculated volume signals the type of respiration is determined in real-time by computing an energy coefficient. Changing breathing patterns can be visualized using a 2-D histogram, which is also used to classify and detect abnormal breathing phases. We evaluated the proposed method on five persons and obtained a reliable differentation of chest- and abdominal breathing in all test cases. Furthermore, we could show that the introduced 2-D histogram enables an accurate determination of changing breathing patterns.

1 Introduction

Improving cancer treatment in radiotherapy is an important topic. To minimize damnification of healthy tissue during treatment sessions techniques like gating or tumor tracking [1, 2] are applied. For so called external gating an adaptive surrogate respiratory signal is used to represent the patient's breathing over time as there is a correlation between the actual tumor movement and the patient's respiration [3].

Independent of the type of an external surrogate signal, there are always uncertainties in the correlation between external surrogates and internal target positions during respiratory cycles. This is mainly caused by the variation of this correlation due to changing breathing patterns and different types of respiration, e.g., chest- or abdominal breathing.

Khamene et al [4] present a method to establish the correlation between a surrogate signal and an internal target prior to the treatment session. Using this method it is possible to compute a mapping between a known reference breathing cycle and the current breathing of a patient. Once the patient changes his type of respiration in any way a new mapping has to be established. Breathing can change in various ways, e.g. chest vs. abdominal breathing or in speed or depth. Detecting all these changes in a respiratory signal requires a fast real-time surface-based method to measure respiratory motion.

Nowadays a common way to acquire a breathing signal is to use a pressure sensor integrated into a belt to generate a 1-D respiratory signal [5]. Another approach is to observe the patient's surface either with or without markers to obtain information about respiration [5, 6]. Unfortunatly most of these systems do not provide the required properties to perform analysis including the just mentioned issues. Recently, a system using an emerging technology called ToF was proposed to measure respiratory motion [7]. Such a system enables marker-less real-time surface monitoring for respiratory motion gating. Furthermore, there are already several other applications within medical imaging where ToF sensors are suggested to improve medical procedures, like 3-D endoscopy or patient positioning [8, 9].

Using a ToF camera it is possible to acquire a 3-D point cloud containing more than 25k points in real-time with 50 Hz and above. ToF cameras emit light in the near infra-red range which is reflected by the surface of an object, e.g., a patient's body. The emitted signal is modulated by a cosine-shaped signal of frequency f. By calculating the phase shift ϕ of both the outgoing and incoming signal, the distance to the camera can be calculated in the following way, where f denotes the modulation frequency of the camera and c is the speed of light:

$$d = \frac{c}{2f} \cdot \frac{\phi}{2\pi} \tag{1}$$

Current available ToF cameras operate at a modulation frequency of about 20 MHz. Thus, the unambiguousness for observable distances of the camera systems is approx. 7.5 m, which is sufficient for respiratory motion tracking.

2 Materials and methods

In the following we will give a brief overview how a ToF sensor enables surface-based respiratory motion classification and verification of multidimensional respiratory signals. Please note, that in the following indices can be considered to be integer values. We denote $\mathbf{P}$ as the $K \times L$ 3-D points of interest acquired by a ToF camera.

$$\mathbf{P} = [\mathbf{p}_{i,j}], i \in \{0, 1, .., K-1\}, j \in \{0, 1, ..L-1\} \tag{2}$$

Furthermore we assume, the ToF camera is rigidly mounted above the patient table. To reduce the amount of data we segment the upper part of the patient's

body using the method described in Schaller et al [9]. As a result for further computations only relevant 3-D points $\hat{\mathbf{P}} \subseteq \mathbf{P}$ ($\subseteq$ denotes a subset of points) have to be considered after the segmentation.

We want to compute a certain region of interest $\mathbf{I} \subseteq \hat{\mathbf{P}}$ and partition this region into n sub-regions $\mathbf{I} = \{\mathbf{S_1} \dot{\cup} \mathbf{S_2} \dot{\cup} .. \dot{\cup} \mathbf{S_n}\}$ and $\mathbf{S_q} \cap \mathbf{S_w} = \emptyset$, where $q \in \{0, 1, .., n-1\}, w \in \{0, 1, .., n-1\}$. Using these n regions of interest we can compute anatomical adaptive respiratory signals of the patient's chest and abdomen. We assume that the coarse orientation of the patient is known and apply a Karhunen-Loève-Transformation to all remaining 3-D points $\hat{\mathbf{P}}$. Resulting, the origin of the coordinate system is placed in the center of gravity of the point cloud $\hat{\mathbf{P}}$ and the axis are aligned with the axial, sagittal and coronal plane of the patient. By applying this transformation an accurate and stable computation of the volume signal can be assured.

To calculate accurate volume signals for each sub-region $\mathbf{S_k}$ ($k \in \{0, 1, .., n-1\}$) each point $\mathbf{p}_{i,j} \in \mathbf{S_k}$ has to be clipped against the 2-D border lines of $\mathbf{S_k}$. This algorithm is necessary to compute the exact volume of each sub-region as the borders of each region intersect the 3-D points arbitrary. We are using the Cohen-Sutherland clipping algorithm to perform this task [10]. By using this approach the partition is always consistent and independent from the patient's position. To calculate the volume of $\mathbf{S_k}$ we take a triangle of three neighboring points $\mathbf{p}_{i,j}$, $\mathbf{p}_{i,j+1}$, $\mathbf{p}_{i+1,j} \in \mathbf{S_k}$ and the distance between the segmentation plane [8] and the mean z-coordinate of these three points to calculate the partial volume. If one or more triangle points are not present in $\mathbf{S_k}$ points computed by the clipping algorithm are used. All particular triangle volumes are summed up to obtain the whole volume value for a specific subregion $\mathbf{S_k}$. By plotting the volume values for each subregion $\mathbf{S_k}$ over time n respiratory graphs can be generated.

We now can use the computed volume signals to distinguish between chest and abdominal breathing. Therefore the signal energy $\mathbf{E_k}$ of each subregion $\mathbf{S_k}$ is calculated over a certain timespan T, where $A_k(t)$ denotes the volume values of subregion $\mathbf{S_k}$.

$$E_k = \sum_{t=-T}^{0} |A_k(t)|^2 \tag{3}$$

After computing the energy for every subregion an energy coefficient α is calculated. Therefore the signal values of the subregions assigned to the chest area E_{chest} and the signal energy of the subregions assigned to the abdominal area $E_{abdominal}$ are summed up. The relation α of the energies is achieved by dividing the abdominal energy by the overall computed energy E_{all}. For the classification an appropriate border λ has to be set:

$$\text{Abdominal Respiration} : \alpha > \lambda \mid \text{Chest Respiration} : \alpha \leq \lambda \tag{4}$$

Furthermore, we analyse the minima and maxima of each volume signal. A 2-D histogram where the time between two minima, which equals the duration of one breathing cycle is plotted on one axis and the maximum amplitude of the

Table 1. α values (in percent) of classification with volume signals for chest and abdominal respiration of five test persons using data acquired by a SR-3000 ToF camera from MESA Imaging.

	1	2	3	4	5
α (chest)	65, 74	37, 62	39, 14	42, 59	64, 77
α (abdominal)	92, 85	91, 40	87, 11	89, 10	81, 30

same breathing cylce on the other axis is computed. Using this visualization, one can immediately detect a variation in the type of breathing of the patient, which is illustrated in more detail in the following.

3 Results

To evaluate the algorithm each part starting with the volume computation was gradually evaluated. Therefore a box with known geometry was placed in front of the camera and was observed from different positions with a distance of 80 cm. We could show, that the difference between the original size of the volume and the computed volume only differs marginal, preconditioned the segmentation prior to the calculation was performed accurately. The real volume of the box was 16368 cm^3, where the computed mean volume was 16501 cm^3 with a standard deviation of 35 cm^3.

Second, the reliability of the classification of chest or abdominal breathing was tested. We computed the signal energy over a time span of 8 sec. Five people were introduced to breath firstly with the thorax and thereafter with the abdomen (Tab. 1). By choosing $\lambda = 0.7$ a distinction between both breathing types in all cases can be achieved.

Finally, a test candidate was advised to perform four different types of breathing, including deep-slow, deep-fast, shallow-slow and shallow-fast breath-

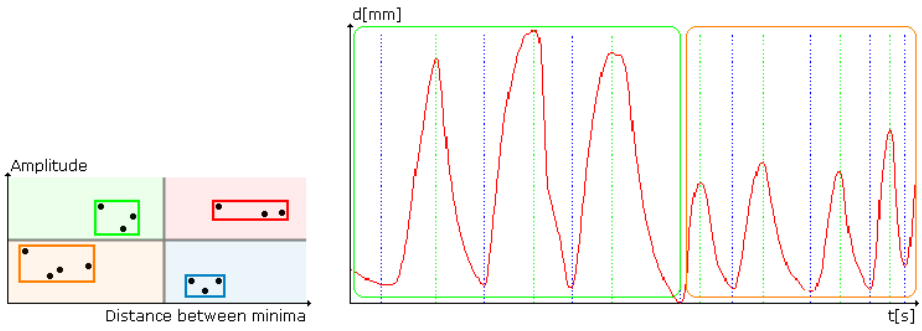

Fig. 1. Left: 2-D histogram showing the cluster formation. right: corresponding breathing cycles for the two left clusters.

ing. While observing the respiration of the test candidate, the above introduced 2-D histogram was successively computed. Figure 1 shows that it is possible to differentiate certain types of breathing. It can be observed, that for regular breathing a clustering in the histogram occurs.

4 Discussion

We introduced a new method to acquire and analyze a respiratory curve using a ToF Camera. The algorithm uses multiple volume signals in order to distinguish between chest and abdominal breathing. Furthermore, using the introduced 2-D histogram, a simple and intuitive way to classify changes in the respiration is introduced. Prospective, further algorithms will be developed to extract more information out of the introduced tools.

Acknowledgement. This work was supported by the International Max Planck Research School for Optics and Imaging (IMPRS-OI), Erlangen, Germany and the SAOT Erlangen, Germany.

References

1. Ue H, Haneishi H, Iwanaga H, et al. Nonlinear motion correction of respiratory-gated lung SPECT images. IEEE Trans Med Imaging. 2006;25(4):486–495.
2. Seppenwoolde Y, Berbeco RI, Nishioka S, et al. Accuracy of tumor motion compensation algorithm from a robotic respiratory tracking system: A simulation study. Med Phys. 2007;34(7):2774–2784.
3. Plathow C, Ley S, Fink C, et al. Analysis of intrathoracic tumor mobility during whole breathing cycle by dynamic MRI. Int J Radiat Oncol Biol Phys. 2004;59(4):952–959.
4. Khamene A, Schaller C, Hornegger J, et al. A novel image based verification method for respiratory motion management in radiation therapy. Proc IEEE ICCV. 2007; p. DVD Proceedings.
5. XA L, Stepaniak C, Gore E. Technical and dosimetric aspects of respiratory gating using a pressure-sensor motion monitoring system. Med Phys. 2006;33(1):145–54.
6. Tarte S, McCelland J, Hughes S, et al. A non-contact method for the acquisition of breathing signals that enable distinction between abdominal and thoracic breathing. Radiother Oncol. 2006;81(1):S209.
7. Schaller C, Penne J, Hornegger J. Time-of-flight sensor for respiratory motion gating. Med Phys. 2008;35(7):1861–6410.
8. Penne J, Höller K, Krüger S, et al. NOTES 3D: Endoscopes learn to see 3-D: Basic algorithms for a novel endoscope. Proc VISAPP. 2007; p. 134–139.
9. Schaller C, Adelt A, Penne J, et al. Time-of-flight sensor for patient positioning. Proc SPIE. 2009; p. online.
10. Foley J, van Dam A, Feiner S, et al. Computer Graphics Principles and Practice. Addison-Wesley Longman Publishing Co; 1996.